

# Risk assessment of hurricane winds for Eglin air force base in northwestern Florida, USA

Kelsey N. Scheitlin · James B. Elsner ·  
Shawn W. Lewers · Jill C. Malmstadt ·  
Thomas H. Jagger

Received: 29 March 2010 / Accepted: 9 December 2010 / Published online: 5 January 2011  
© Springer-Verlag 2011

**Abstract** Hurricane winds present a significant hazard for coastal infrastructure. An estimate of the local risk of extreme wind speeds is made using a new method that combines historical hurricane records with a deterministic wind field model. The method is applied to Santa Rosa Island located in the northwestern panhandle region of Florida, USA. Firstly, a hurricane track is created for a landfall location on the island that represents the worst-case scenario for Eglin Air Force Base (EAFB). The track is based on averaging the paths of historical hurricanes in the vicinity of the landfall location. Secondly, an extreme-value statistical model is used to estimate 100-year wind speeds at locations along the average track based again on historical hurricanes in the vicinity of the track locations. Thirdly, the 100-year wind speeds together with information about hurricane size and forward speed are used as input to the HAZUS hurricane wind field model to produce a wind swath across EAFB. Results show a 100-year hurricane wind gust on Santa Rosa Island of  $58 (\pm 5) \text{ m s}^{-1}$  (90% CI). A 100-year wind gust at the same location based on a 105-year simulation of hurricanes is lower at  $55 \text{ m s}^{-1}$ , but within the 90% confidence limits. Based on structural damage functions and building stock data for the region, the 100-year hurricane wind swath results in \$574 million total loss to residential and commercial buildings, not including military infrastructure, with 25% of all buildings receiving at least some damage. This methodology may be applied to other coastal areas and adapted to predict extreme winds and their impacts under climate variability and change.

## 1 Introduction

Hurricanes cause an average of \$10 billion in damage in the USA annually. In 2004 and 2005, the damage totaled \$150 billion. Approximately 85% of US hurricane damage comes from major hurricanes (category 3 or higher on the Saffir Simpson hurricane scale), while they comprise only 24% of landfalling hurricanes (Pielke Jr. et al. 2008). A noted increase in the intensity of the strongest hurricanes in recent times (Elsner et al. 2008b) is of particular concern for estimates of future losses 100 years from now.

The frequency of hurricane strikes and the amount of damage they cause varies by location. The occurrence and magnitude of historical hurricanes can be used to estimate the return period of wind speeds exceeding a specified threshold. The return period (roughly the average time between successive events) can be made local by extrapolation (Elsner et al. 2008a). Damage estimates are more complicated and must take into account location-specific vulnerability. Interannual variability in hurricane frequency and damage losses at the coast are related to ocean temperature, the El Niño Southern Oscillation, the North Atlantic Oscillation, and solar activity (Elsner et al. 1999; Pielke Jr. and Landsea 1999; Elsner and Jagger 2004, 2006; Jagger et al. 2008; Hodges and Elsner 2010).

The potential for a particular hurricane to cause damage depends on the strength of its winds, its forward speed, and its geographic size. For a given landfall location, the damage potential also depends on local population and economy. Here, we fix this location and consider the distribution of hurricane characteristics along an average track, producing a track-relative climatology. In short, historical hurricane tracks are used to construct a “mean” hurricane track for a given coastal location. We then consider the distribution of hurricane characteristics as the

K. N. Scheitlin (✉) · J. B. Elsner · S. W. Lewers ·  
J. C. Malmstadt · T. H. Jagger  
Florida State University,  
Tallahassee, FL, USA  
e-mail: kscheitlin@fsu.edu

storm approaches the shore, displaying the characteristics as profiles along the average track. The characteristics are used to model a wind swath and damage estimates using HAZUS. The approach of combining a statistical model with a deterministic model was illustrated recently for assessing the risk of storm surge in New York City (Lin et al. 2010).

Our geographic focus is the Eglin Air Force Base (EAFB) located in panhandle region of Florida (Fig. 1) and represents a first step toward investigating the effects of near-term (next 100 years) risk to military infrastructure located in low coastal or near-coastal areas due to predicted changes in climate and sea level. Models project global sea level rises over the next 100 years on the order of 1 m or more, which will increase hurricane storm surge penetration (Mousavi et al. 2010). As a result, EAFB and similarly situated coastal military facilities will likely experience significant changes to environmental resources and artificial infrastructure. Shoreline retreat, increased flooding and erosion, and greater wind loads and storm surge will all contribute to increased losses. This work focuses on the threat of extreme hurricane winds based on the current climate, with particular emphasis on the 100-year event.

The paper is divided into three parts: the construction of an average “worst case” hurricane track, the determination of hurricane characteristics along this track, and the simulation of hurricane wind gusts and damage losses using HAZUS. Section 2 describes the data used to construct the “worst-case” track and to accumulate hurricane characteristics. Section 3 details the generation of the track for EAFB by using distance maps. In Section 4, the track is represented by equal-interval points, for which hurricane characteristics representing the 100-year event are found. These characteristics are shown as profiles along the track. In Section 5, a subset of hurricane characteristics, referred to as hurricane

vitals, are used to simulate a 100-year hurricane event for EAFB. HAZUS provides the wind swath and damage estimates. The 100-year wind gust over Santa Rosa Island estimated from thousands of hurricane simulations compares favorably with the wind gust estimated by our simpler approach. Section 6 provides a summary and conclusion.

## 2 Hurricane data

Hurricane loss models are important for insurance, financial, and government sectors to estimate damage losses. These models require several subcomponents, including wind and vulnerability models, and a hurricane climatology for the specific area. The hurricane climatology is often based off the historical record, providing information about the recurrence rate and characteristics of past hurricanes (Watson and Johnson 2008).

Past hurricane data are acquired from the Hurricane Database (HURDAT; best track) maintained by the National Hurricane Center. HURDAT contains data for tropical cyclones observed in the Atlantic Ocean, Gulf of Mexico, and Caribbean Sea since 1851. Here we use a version of HURDAT containing hourly interpolations of tropical cyclones from 1851–2008, as constructed in Jagger and Elsner (2006). The historical hurricanes are used to create the average track and obtain climatological hurricane characteristics. Additionally, data from Demuth et al. (2006) are used for information on hurricane size.

The present work expands the idea of a hurricane climatology to include a track-relative climatology of hurricane characteristics specific to a given location. In other words, we seek to provide climatological hurricane characteristics along a track based on local historical hurricanes. The hurricane characteristics are subsequently used to model an extreme hurricane wind event affecting EAFB. Therefore, our interest is in a track that would likely produce a worst-case scenario for EAFB and threaten military infrastructure.

For several reasons, the largest threat to EAFB is a hurricane striking the western side of the base, with much of the base on the immediate eastern side of the track. Keim et al. (2007) show that for average- or large-size hurricanes, the maximum winds extend forward and to the right about 50–100 km from the eye. This encompasses an area twice as large as the area of winds to the left of the eye. Wind speeds on the forward-right quadrant of the storm are also greater due to the cumulative effect of the hurricane wind speed about the circulation and the forward motion of the tropical cyclone (Elsner and Kara 1999). The stronger winds on the right side increase the storm surge (Simpson and Riehl 1981). Tornadoes (Pearson and Sadowski 1965) and lightning (Corbosiero and Molinari 2003) are also more common in this forward-right quadrant of a landfalling hurricane.

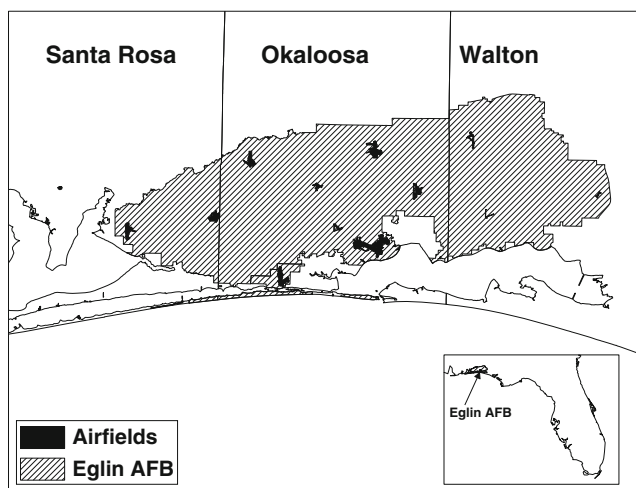


**Fig. 1** Study area. Eglin Air Force Base (*striped*) is located in the Florida Panhandle, comprising of portions of Santa Rosa, Okaloosa, and Walton counties

The landfall location chosen for the average EAFB track is situated at 30.4° N and 86.8° W, on Santa Rosa Island, Florida. This point is located approximately 30 km southwest of the geographic centroid of EAFB, in the western portion of the base property. A hurricane making landfall here places much of EAFB in the most destructive portion of the hurricane. This location is a worst-case landfall scenario for the base and is the fiducial landfall point for the track-relative climatology.

Next, we create an average track for the worst-case landfall location by examining historical hurricanes making landfall near the fiducial point. Hourly interpolated data are used to find the strongest hurricanes in history that passed nearby. Each of these cyclones reached major hurricane intensity within 150 km of the fiducial point. In Fig. 2, the tracks are ranked according to their average great-circle distance from that point, shown by greyscaling. Table 1 lists attributes for the corresponding hurricanes, including year, name (once naming of tropical cyclones was implemented), and distance to the fiducial point. In the next section, we describe a method to create an average track from these ten tracks. The average track creates a realistic and “most-likely” scenario for an extreme EAFB event by basing the hurricane’s track on climatological hurricane behavior (i.e., the typical EAFB track) while maximizing its destructive potential. Track averaging also maintains methodological consistency, as other extreme event characteristics are determined using climatological values.

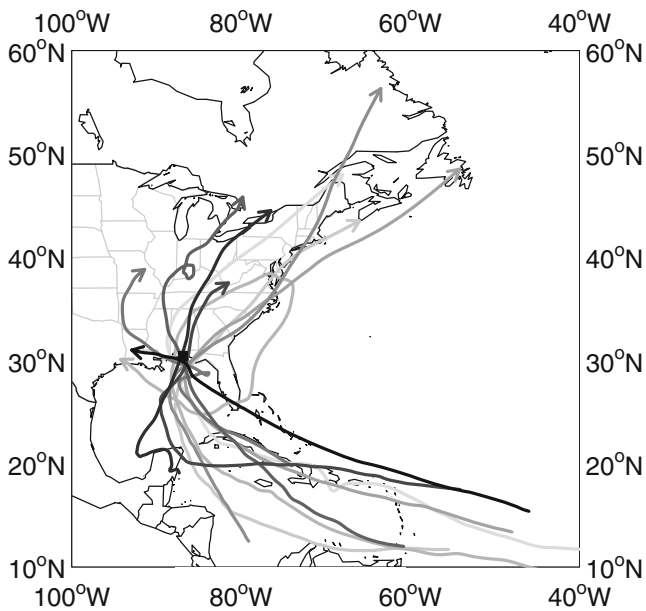


**Fig. 2** Tracks of the ten major hurricanes passing within 150 km of the fiducial point over the period 1851–2008. The fiducial point represents a worst-case landfall scenario for the Eglin Air Force Base. The gray scale on the tracks corresponds to the distance from the fiducial point, with the darker tracks indicating closer approaches

**Table 1** Hurricanes passing within 150 km of the fiducial point over the period 1851–2008

Year	Name	Distance (km)
1926	Not named	57
1995	Opal	67
1975	Eloise	74
2005	Dennis	85
1985	Elena	87
1894	Not named	92
1851	Not named	105
2004	Ivan	114
1877	Not named	130
1979	Frederic	133

The maximum sustained wind of the hurricane when it passed within 150 km exceeded 50 m s<sup>-1</sup> (at least a category 3 on the Saffir/Simpson hurricane scale). The distance (km) is the hurricane’s closest approach to the fiducial point. Hurricanes were not named before 1950

### 3 An average hurricane track

There are various ways to determine an average track from a set of hurricanes making landfall at a particular location. Our method uses the inverse-distance weighted (IDW) average of a series of distance maps. The method is presented in detail in Scheitlin et al. (2010). This method weights the particular hurricane track inversely to the distance between the hurricane’s closest approach to the fiducial point. In other words, the hurricanes tracking nearest the fiducial point have the most influence on the average track.

A distance map is made for each of the tracks in Fig. 2. On each distance map, distances to the corresponding track are computed on a common 0.1° longitude grid. The track itself has a value of zero, with distances increasing away from the track. The distances are given in degrees of longitude. The ten distance maps ( $D_k(s)$ , for  $k=1, \dots, 10$ ) are subsequently averaged using IDW, so that the average distance map is weighted towards the tracks that are closest to the fiducial point. The formula for the average distance map,  $D(s)$ , using IDW is

$$D(s) = \frac{\sum_{k=1}^{10} w_k D_k(s)}{\sum_{k=1}^{10} w_k} \tag{1}$$

where

$$w_k = \frac{1}{d(e, t_k)} \tag{2}$$

and  $d(e, t_k)$  is the nearest great-circle distance from the fiducial point ( $e$ ) to the track ( $t_k$ ).

The average distance map is shown in Fig. 3 with contour masks representing the weighted–averaged distance of the strongest hurricanes closest to EAFB. The outermost contour encompasses the area that has average distances less than  $3.0^\circ$  of longitude and the innermost contour encompasses the area that has average distances less than  $0.75^\circ$ . Contours are shown at  $0.25^\circ$  intervals. This geovisualization of the combined set of tracks provides some information about the spatial distribution of intense hurricanes affecting the area. The contour gradient in the direction of the track is tighter post-landfall than pre-landfall. This indicates that past EAFB hurricanes have more in common prior to landfall than after. One reason for this could be the susceptibility of a decaying hurricane post-landfall to be controlled by the variable synoptic conditions. In contrast, stronger hurricanes will follow a more predictable manner based on larger-scale climate forcing. Drawing a line through the shortest distances on the average distance map and perpendicular to the contours provides an average hurricane track (Scheitlin et al. 2010).

The average distance map is relatively insensitive to the number of hurricanes chosen, which is a function of the distance threshold used to select the hurricanes. This can be seen by repeating the analysis using a search radius twice as large (300 km). This increases the sample size from 10 to 24 hurricanes. The track having the greatest distance to the fiducial point increases from 33 km using the set of ten hurricanes to 274 km with the larger set of 24 hurricanes, but the average distant maps are quite similar. This insensitivity is a consequence of the inverse-distance weighting scheme. For this paper, we use the track corresponding to the smaller sample size.

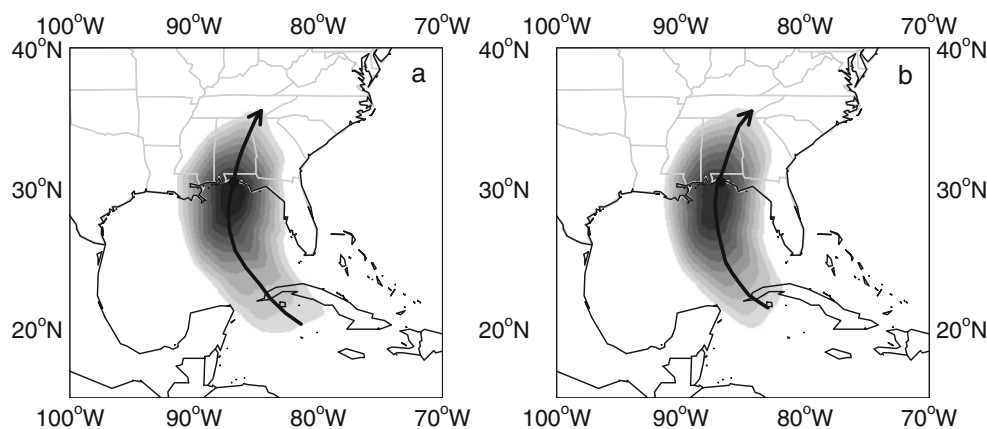


**Fig. 3** Average distance maps. The maps are based on using the (a) ten and (b) 24 major hurricanes passing closest to the fiducial point over the period 1851–2008. Contours indicate the weighted average distance of the set of hurricanes. The outer contour encompasses the area that has an average distance less than  $3^\circ$  of latitude and the inner

#### 4 Hurricane characteristics along the track

Next we add hurricane characteristics to the average track for EAFB. This is done at equally spaced points along the track, including the fiducial landfall point (Fig. 4). We use a spacing of 100 km and since we are interested in the hurricane before and directly after landfall, we use the portion of the track covering its movement across the Gulf and its initial inland penetration. The number of track locations is arbitrary but using a 100-km spacing ensures some uniformity in wind speeds.

Hurricane characteristics are obtained for the purpose of creating an EAFB track-relative climatology, and for simulating an extreme EAFB hurricane event in HAZUS. The model requires a set of values along a prescribed track that characterize the hurricane. These values, called “vitals,” include information about location, intensity, forward speed, size, central pressure and wind speed decay. The vitals are obtained from historical data and known empirical relationships as described below.

##### 4.1 One-hundred-year wind speeds

Total damage depends to a large degree on the hurricane’s maximum wind speed. Maximum wind speed refers to the estimated strongest (10 m, 1 min sustained) winds somewhere in the eyewall of the hurricane. The strongest winds are typically found on the right side of the hurricane track when looking in the direction of the storm’s forward motion. The radial distance from the center of circulation to the location of the strongest winds is called the radius to maximum winds ( $R_{MW}$ ) and is, on average, 35 km for hurricanes over the Gulf of Mexico (Vickery and Wadhera 2008).

contour encompasses the area that has an average distance less than  $0.75^\circ$ , with a  $0.25^\circ$  contour interval. The average track is a *line* through the shortest distances on the average distance map and perpendicular to the contours

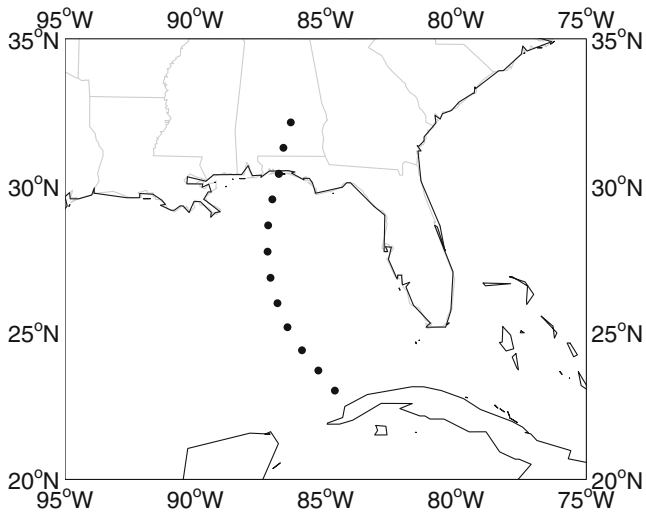


**Fig. 4** Points along the average EAFB hurricane track. Points are equally spaced at 100-km intervals from the fiducial landfall point. Hurricane characteristics are determined at these locations to create a track-relative climatology

Our interest is in the highest wind speed that can be expected, on average, in any 100-year interval for locations along the track. Under the assumption that the maximum wind speed of any hurricane occurs within 35 km of the center we collect hurricanes that have come within this distance of a particular location. We then rank the hurricane wind speeds from fastest to slowest and determine the parameters of an extreme-value distribution. However the historical record of hurricanes is too short to have many such hurricanes, so we search at larger distances allowing us to find more hurricanes and to accurately estimate the statistical parameters of the distribution. Linear regressions of the distribution parameters on search radius allow us to estimate the parameters at the 35-km radius. These estimated parameters are subsequently used to determine the highest wind speed that can be expected within the 35-km radius in any 50-year interval. This 50-year return-level wind speed is used as the 100-year return-level wind speed based on the assumption that the strongest winds are typically on the right side of the hurricane track and it is just as likely for a hurricane to track to the right of the location as it is to track to the left of the location. The method is developed and described in Elsner et al. (2008a) and applied to Florida cities in Malmstadt et al. (2010).

The above procedure for estimating the 100-year wind speed at a location is repeated independently for all locations along the track with results shown in Fig. 5. The points indicate the estimated 100-year return-level wind speed. The 90% confidence interval about this estimate is indicated by the vertical line. The set of locations is along

the track (shown by black circles in panel b) with the distance prior to, and after, landfall marked along the horizontal axis. The peak 100-year sustained wind speed is  $58 \text{ m s}^{-1}$  at the location along the track 600 km before landfall. At landfall, the 100-year wind speed is  $48 \text{ m s}^{-1}$  with a 90% confidence interval on this estimate between  $44$  and  $51 \text{ m s}^{-1}$ .

The 100-year wind speeds are strongest for locations prior to landfall and get weaker as the locations get closer to the coast. The weakest winds occur over land. Based on the historical record of hurricanes in the northern Gulf of Mexico, EAFB can expect an approaching strong hurricane to begin decaying approximately 550 km from landfall. Thus if the hurricane maintains a forward speed of  $6.5 \text{ m s}^{-1}$ , the weakening begins about 1 day before the time of landfall.

The tendency for pre-landfall weakening is common to hurricanes in the Gulf of Mexico, but its cause has received less attention than the more relevant concern of inland hurricane decay (Kaplan and DeMaria 1995, 2001). Vickery and Wadhera (2008) suggest that tropical cyclones in the Gulf of Mexico exhibit a weakening 6–24 h prior to landfall that is not exhibited in hurricanes striking other parts of the US coast. This weakening is characterized by an increase in central pressure  $p$  and an increase in the  $R_{MW}$ , creating a more uniform distribution of the pressure gradient force across the diameter of the hurricane.

Information on Hurricane Opal of 1995 is shown in Fig. 5 for comparison. Opal took a track farther to the west as it approached the base than the average EAFB track (see Fig. 5b) although the landfall locations are only 30 km apart. We interpolate the Opal's hourly wind speed values to the 100-km-spaced pre- and post-landfall locations. The wind speed profiles are similar, although our extreme hurricane generally has higher wind especially at large distances from the coast. Opal intensified rather rapidly reaching a wind speed of  $60 \text{ m s}^{-1}$  (Powell and Houston, 1998) over a ring of very warm surface and thermocline waters over the northern Gulf approximately 450 km from the coast (Hong et al. 2000). Opal decayed just as rapidly, making landfall with  $42 \text{ m s}^{-1}$  winds. This speed is just below the 90% confidence interval of the 100-year return level. Opal's intensity values were used in creating the 100-year return levels.

Likely causes for pre-landfall decay of hurricanes in this region include movement away from the warm core ring, entrainment of dry continental air (Levinson et al. 2009), and the interaction of continental aerosols (Khain et al. 2008). Opal's more dramatic decay could have resulted from enhanced advective mixing of dry continental air due to an upper-level trough over the coast (Shay et al. 2000).

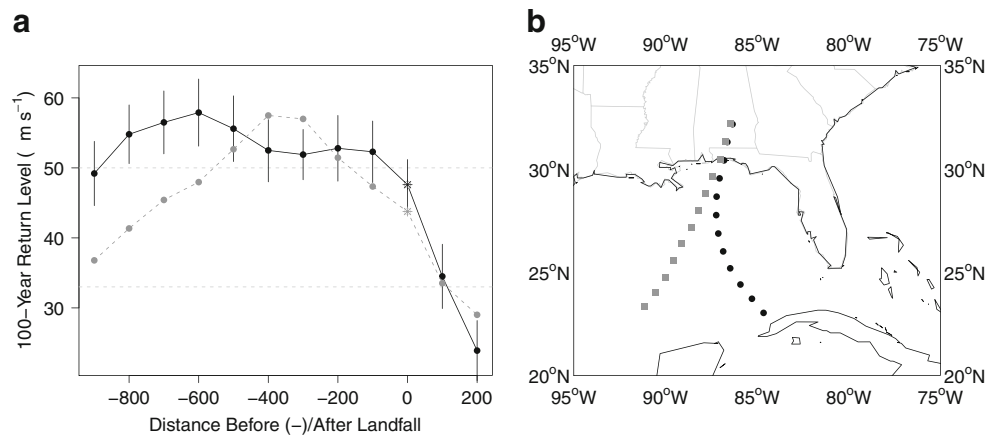


**Fig. 5** Intensities and tracks of the extreme event and Hurricane Opal. **a** Wind speed ( $\text{m s}^{-1}$ ) profiles of the extreme event (black) and Hurricane Opal (grey) along their respective tracks. Landfall values are marked with an asterisk. Values are given at 100-km intervals, with distances in kilometers before (negative) and after landfall plotted on the horizontal axis. The 100-year return levels are for a 35-km

radius around the given point. Return levels are calculated using an application of Elsner et al. (2008a). The vertical lines are the 90% confidence interval. Wind speeds for Opal are the value of the closest 1-h observation. **b** Equal-interval points along the track of the extreme event (black) and Hurricane Opal (grey)

#### 4.2 Forward speed

The amount of hurricane damage at a given location depends also on the amount of time the wind blows, which is a function of the hurricane's forward speed and size. A hurricane moving slower over an area will cause more damage than a hurricane moving faster, all else being equal. The forward speed of hurricanes passing within a 100-km radius of the locations is used to compute an average. If a hurricane has more than one observation in the search radius, the maximum observed value is used in the calculation. The search domain for the location 300 km from landfall and the average translational speed as a function of distance along the track are shown in Fig. 6. Results show that, on average, hurricanes approaching EAFB move at speeds of  $6\text{--}7 \text{ m s}^{-1}$  with a slight acceleration

prior to landfall. After landfall there is a significant increase in forward velocity as the hurricanes get pushed northward and eastward under the influence of the mid-latitude jet streams.

#### 4.3 Radius to maximum winds

The size of a hurricane is characterized by the  $R_{\text{MW}}$ . Formally,  $R_{\text{MW}}$  is defined as the distance from the center of the cyclone to the farthest extension of the maximum wind speeds. A typical  $R_{\text{MW}}$  is 30–50 km (Hsu and Yan 1998). Vickery and Wadhera (2008) note that in the Gulf of Mexico there is no statistically significant relationship between  $R_{\text{MW}}$  and latitude or  $\Delta p$ , which is the difference in the cyclone's central and peripheral pressures. Thus, the

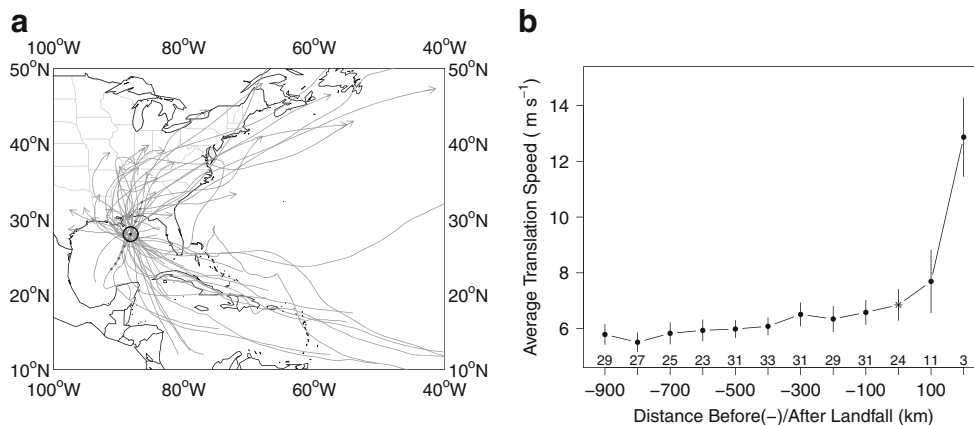


**Fig. 6** Track selection and forward speeds. **a** Tracks of the 34 hurricanes passing within a 100-km great-circle distance of the track point 300 km from the landfall location. The forward speed of each hurricane as it passed within 100 km of the location is used to

compute the average. **b** Average forward speeds ( $\text{m s}^{-1}$ ) as a function of distance before and after landfall. Vertical bars indicate the  $\pm$  on standard errors above the mean speed. The number of hurricanes used in the averaging are shown above the horizontal axis

$R_{MW}$  cannot be approximated using any of the information already obtained. Vickery and Wadhera (2008) note three traits of Gulf of Mexico landfalling hurricanes. Firstly, the average  $R_{MW}$  is estimated to be 35 km. Secondly, there is a notable change in  $R_{MW}$  associated with the decay of Gulf hurricanes as they approach the coast. Finally, Gulf of Mexico landfalling hurricanes are smaller, on average, than their Atlantic coast counterparts.

To check these relationships in our study area, we obtain  $R_{MW}$  data from the extended best-track database (Demuth et al. 2006). The database contains information for most North Atlantic tropical cyclones since 1988. For 1988 and 1989, the data are from the vortex messages of aircraft reconnaissance missions. For 1990–present, the data are from the National Hurricane Center archives, estimated from operational data sources including ship reports, aircraft reconnaissance data and satellite imagery. Information is provided at 6-h intervals. We focus on major hurricanes estimates within a region of the northern Gulf of Mexico off the coast of EAFB. Within this region the average  $R_{MW}$  is 33 km with a standard error of 12 km. As Vickery and Wadhera (2008) suggest, there is no significant correlation between  $R_{MW}$  and maximum wind speeds, or  $R_{MW}$  and latitude. Thus, we use the Vickery and Wadhera (2008) estimation of 35 km as a constant  $R_{MW}$  through the length of the track.

#### 4.4 Holland $B$ pressure profile parameter

The slackening of the winds at distances from the hurricane center beyond the  $R_{MW}$  is described by the Holland  $B$  parameter. Specifically, Holland  $B$ , with nondimensional values ranging between 1 and 2.5, dictates the shape of the

surface air pressure field of a hurricane. Holding  $R_{MW}$  and central pressure constant, a decrease in  $B$  indicates a weaker maximum wind speed with more dispersed pressure gradients across the wind field (Holland 1980). In other words, after the hurricane reaches its peak wind speed, wind speeds gradually decrease away from the eyewall in a nonlinear fashion. Thus a lower value of  $B$ , all else being the same, indicates a larger area subjected to the strongest winds, but the maximum wind speed is relatively weaker. Constant pressure and  $R_{MW}$  with a higher value of  $B$  cause a higher maximum wind speed but a quicker decrease in velocity beyond the  $R_{MW}$ .

Vickery and Wadhera (2008) provide the following empirical formula for Holland  $B$  for landfalling hurricanes based on observations of  $R_{MW}$  and latitude ( $\phi$ ):

$$B = 1.811 - 0.00557R_{MW} - 0.01295\phi \tag{3}$$

This equation is used at each of our track locations. The values of  $B$  range from 1.32 at the first location to 1.20 at the location farthest inland.

The complete set of vitals for each track location is listed in Table 2. The list is ordered by location along the track from farthest from coast to farthest inland. The minimum central pressure values are obtained from the wind-pressure relationship of Brown et al. (2006) for Gulf of Mexico hurricanes. The “Inland” tag is set to 1 for locations over land.

### 5 Estimates of wind speeds and wind damage losses from HAZUS

Hurricane wind damage results from winds circulating through the storm as it moves inland. HAZUS constructs a

**Table 2** Vitals for an extreme hurricane affecting EAFB

$\phi$	$\lambda$	Wind speed (m s <sup>-1</sup> )	Forward speed (m s <sup>-1</sup> )	$R_{MW}$ (km)	Central pressure (mb)	Holland $B$	Inland
23.0	-84.6	49.2	5.8	35	960.7	1.32	0
23.7	-85.3	54.8	5.5	35	949.8	1.31	0
24.4	-85.9	56.5	5.8	35	946.4	1.30	0
25.2	-86.5	57.9	6.0	35	943.5	1.29	0
26.0	-86.9	55.6	6.1	35	948.2	1.28	0
26.9	-87.1	52.5	6.1	35	954.4	1.27	0
27.8	-87.2	51.9	6.5	35	955.6	1.26	0
28.6	-87.2	52.8	6.3	35	953.8	1.25	0
29.5	-87.0	52.3	6.6	35	954.8	1.23	0
30.4	-86.8	47.6	6.8	35	963.6	1.22	1
31.3	-86.6	34.5	7.7	35	985.0	1.21	1
32.2	-86.3	23.9	12.9	35	998.6	1.20	1

The latitude ( $\lambda$ ) and longitude ( $\phi$ ) are those of the equal-interval points along the average track. The wind speed (m s<sup>-1</sup>) refers to the 100-year return level for that point. The translation speed (m s<sup>-1</sup>), radius of maximum winds ( $R_{MW}$ ; km), pressure (mb), and Holland  $B$  profile parameter are obtained from past hurricanes and formulas based on known relationships. The inland column is a binary variable describing whether the point is over water (0) or land (1). These vitals are used as input to HAZUS to produce a wind field

two-dimensional wind field associated with a hurricane based on a set of vitals. As the vitals change along the track so does the wind field. The vitals can be provided by a user (deterministic mode), or intrinsic to HAZUS based on a historical event (historical mode) or a collection of simulated (synthetic) hurricane events (probabilistic mode). In each mode, HAZUS uses the set of wind fields to generate a wind swath containing the fastest winds at any location and a resulting set of damages and loss estimates.

HAZUS was developed in the early 1990s, and the hurricane component was added in 1997. It was released for research purposes in 2005 (Schneider and Schauer 2006) and it continues with periodic updates. Here we use version MR4 to generate a wind swath and loss estimates from the set of vitals (Table 2). We also compare 100-year wind gusts at a particular location using the probabilistic mode.

### 5.1 Wind speeds

We gather hurricane wind information using the HAZUS deterministic and probabilistic modes. In the deterministic mode, a single set of user-defined vitals is used to generate a wind swath across the area of interest. In the probabilistic mode, hundreds of hurricane vital sets are generated from a 105-year simulation of hurricanes across the North Atlantic basin.

Each vital set is used to create a wind field, and the set of winds is used to estimate return-level wind speeds for each census tract. The probabilistic results are available as a table of return levels.

The HAZUS wind field generation is described in detail in Vickery et al. (2000a,b). All wind swaths created from a set hurricane vitals (whether deterministic or probabilistic) are done in the same way. Wind estimates are made using two model components; the hurricane hazard model and the terrain model. The hurricane hazard model uses the hurricane vitals to create wind fields through the length of the track. The terrain model alters the wind fields based on local terrain. Greater friction associated with a rougher land surface causes a weakening of the average wind speeds. Peak wind gusts on the other hand are less affected by surface roughness (Zhu, 2008). HAZUS incorporates a wind speed-surface roughness relationship with the terrain information from land use land cover (LULC) maps. The set of wind fields from these models result in a wind swath of the maximum winds affecting particular geographic locations.

Here, we compare the HAZUS wind swath generated in deterministic mode from our 100-year wind speed along the average track with the HAZUS 100-year wind speed generated in probabilistic mode. A comparison of maximum wind gusts is made at the census tract containing the landfall location (Fig. 7). The probabilistic return-level

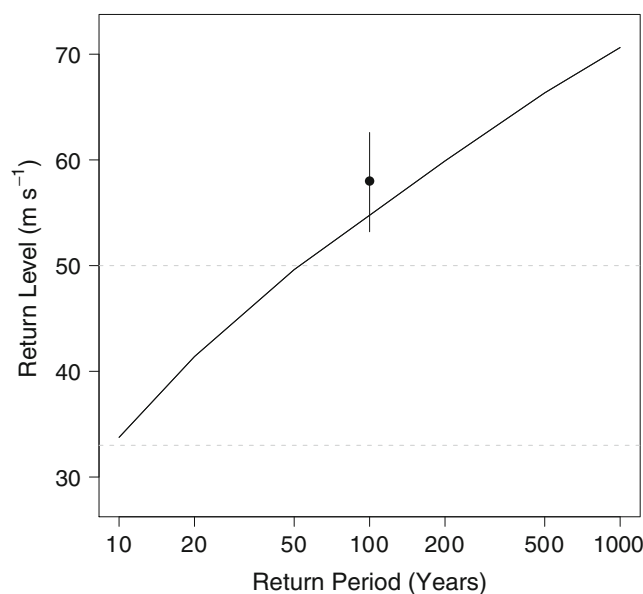


**Fig. 7** Wind speed gusts for the Santa Rosa Island census tract. The curve shows 100-year return levels of wind gusts from the HAZUS probabilistic output. The points and error bars are from the HAZUS deterministic output using our extreme hurricane vitals for EAFB

curve represents wind gusts of this magnitude or higher at the geographic centroid of the tract on average once every return period. The deterministic information is gathered from the wind swath resulting from our hurricane vitals.

Our deterministic wind swath shows a 100-year wind gust estimate of  $58 \text{ m s}^{-1}$ . We obtain the 90% confidence intervals ( $53\text{--}63 \text{ m s}^{-1}$ ) on this estimate by running similar deterministic hurricanes, with intensity values at the lower and upper 90% confidence limits from Fig. 5. This is compared to the probabilistic 100-year gust of  $55 \text{ m s}^{-1}$ , which is within the 90% confidence limits of our estimate. As noted, the probabilistic 100-year wind gust is based on a probabilistic Monte Carlo simulation of 105 years of hurricanes across the North Atlantic.

### 5.2 Total wind damage

Given the spatial variation of hurricane winds, HAZUS produces wind-loss estimates at the census tract level. It does this by combining three models—a wind load model, a physical damage model, and an economic loss model—and information on building types and materials from census data.

The wind load model includes wind pressure modeling, and wind-borne debris modeling. The wind pressure model uses empirical data from wind tunnel tests to estimate directionally dependent wind-induced pressures (Vickery et al. 2006a). Wind pressures are important due to their strain on buildings, resulting in building damage and causing wind-borne debris. Wind-borne debris modeling is a critical

component of a physical damage model. HAZUS has two debris models: one for residential debris, and another for roof gravel, which acts as a missile during high winds. The wind load model provides information to estimate wind-induced damage and loss (Vickery et al. 2006a).

Using detailed building stock information, the physical damage model estimates the damage associated with the given wind load. The physical damage model predicts the failure of building components due to progressive failures, internal pressures, duration effects, and changes in wind direction and speed. The model focuses on damage to the exterior of the buildings, including the windows, roof cover, roof deck, joint failures, and wall failures. Five damage states are used to describe the amount of damage to each of the buildings (Vickery et al. 2006b).

The economic loss model uses the information from the physical damage model to estimate hurricane wind-induced losses. It is important to note that losses from storm surge or any other source are not included. Specifically, the economic loss model takes into account actual building losses, loss of contents and inventory, and loss of building use (Vickery et al. 2006b). The model does not contain data for military building stock, but provides damage estimates for residential and commercial buildings. HAZUS provides a basis for assessing the military infrastructure wind damage losses, and the military building stock information may be added as a separate component.

HAZUS estimates building-related wind damage of over \$573 million the study region (consisting of Okaloosa, Walton and Santa Rosa counties) for the 100-year deterministic event. The model estimates that 461 households will be displaced due to the hurricane and require a temporary shelter. Approximately one fourth of all building are expected to have some type of damage, providing an estimated three million tons of debris. This amount of debris would require 3,359 truckloads for removal.

## 6 Summary and conclusions

This paper demonstrates a new method for estimating the risk of local extreme winds that combines historical hurricane records with a deterministic wind field model. Firstly, a hurricane track is created for a landfall location on the island that represents a worst-case scenario. The track is based on averaging the paths of historical hurricanes in the vicinity of the landfall location. Secondly, an extreme-value statistical model is used estimate 100-year wind speeds at locations along the average track again based on historical hurricanes in the vicinity of the track locations. The locations are separated along the track at 100-km intervals. Thirdly, the 100-year wind speeds together with information about hurricane size ( $R_{MW}$ , and the Holland  $B$  parameter) and forward speeds are

used as input to the HAZUS hurricane wind field model to produce a wind swath. The  $R_{MW}$  is a constant 35 km along the track and the weakening of winds beyond the  $R_{MW}$  are characterized by the Holland  $B$  parameter.

The procedure produces a 100-year hurricane wind gust on Santa Rosa Island of  $58 (\pm 5) \text{ m s}^{-1}$  (90% CI). An estimated 100-year wind gust at the same location based on a 105 year simulation of hurricanes is lower at  $55 \text{ m s}^{-1}$ , but within the 90% confidence limits. Based on structural damage functions and building stock data for the region contained in HAZUS, the 100-year hurricane wind swath results in \$574 million total loss to residential and commercial buildings, not including military infrastructure, with 25% of all buildings receiving at least some damage.

The 100-year wind gust estimated with our approach, while somewhat higher, has a 90% confidence interval that includes the 100-year wind gust estimated from the HAZUS simulation. However, the real strength of our approach is that it requires many fewer parameters than the probabilistic approach, making it useful for considering questions associated with climate variability and climate change. For instance, the extreme-value model parameters can be regressed on ocean temperature providing a way to condition the 100-year wind speed (and damage potential) on a future climate featuring warmer oceans. The methodology can be applied to other coastal regions.

**Acknowledgments** This work was done as part of the lead author's dissertation with support from Florida State University, USA. Additional support came from the US Department of Defense, through the Strategic Environmental Research and Development Program (SERDP), Project SI-1700, as well as from the US NSF (ATM-0738172). Views expressed within do not necessarily reflect the opinions of the funding agency. All statistical analyses were performed using the software environment R (<http://www.r-project.org>).

## References

- Brown DP, Franklin JL, Landsea C (2006) A fresh look at tropical cyclone pressure-wind relationships using recent reconnaissance based 'best track' data (1998–2005). In: Preprints 27th Conference on Hurricanes and Tropical Meteorology. American Meteorological Society, Orlando, Florida
- Corbosiero KL, Molinari J (2003) The relationship between storm motion, vertical wind shear, and convective asymmetries in tropical cyclones. *J Atmos Sci* 60:366–376
- Demuth JL, DeMaria M, Knaff JA (2006) Improvement of advanced microwave sounding unit tropical cyclone intensity and size estimation algorithms. *J Appl Meteorol* 45:1573–1581
- Elsner JB, Jagger TH (2004) A hierarchical Bayesian approach to seasonal hurricane modeling. *J Climate* 17:2813–2827
- Elsner JB, Jagger TH (2006) Prediction models for annual U.S. hurricane counts. *J Climate* 19:2935–2952
- Elsner JB, Kara AB (1999) Hurricanes of the North Atlantic: climate and society. Oxford University Press, Oxford
- Elsner JB, Kara AB, Owens MA (1999) Fluctuations in North Atlantic hurricane frequency. *J Climate* 12:427–437

- Elsner JB, Jagger TH, Liu K (2008a) Comparison of hurricane return levels using historical and geological records. *J Appl Meteor Climatol* 47:368–374
- Elsner JB, Kossin J, Jagger TH (2008b) The increasing intensity of the strongest tropical cyclones. *Nature* 455:92–95
- Hodges RE, Elsner JB (2010) Evidence linking solar variability with US hurricanes. *Int J Climatol*. doi:10.1002/joc.2196
- Holland GJ (1980) An analytical model of the wind and pressure profiles in hurricanes. *Mon Weather Rev* 108:1212–1218
- Hong X, Chang SW, Raman S, Shay LK, Hodur R (2000) The interaction between Hurricane Opal (1995) and a warm core ring in the Gulf of Mexico. *Mon Weather Rev* 128:1347–1365
- Hsu SA, Yan Z (1998) A note on the radius of maximum winds for hurricanes. *J Coast Res* 14:667–668
- Jagger T, Elsner J (2006) Climatology models for extreme hurricane winds in the United States. *J Climate* 19:3220–3236
- Jagger TH, Elsner JB, Saunders MA (2008) Forecasting U.S. insured hurricane losses. In: Diaz H, Murnane R (eds) *Climate extremes and society*. Cambridge University Press, Cambridge, pp 189–208
- Kaplan J, DeMaria M (1995) A simple empirical model for predicting the decay of tropical cyclone winds after landfall. *J Appl Meteorol* 34:2499–2512
- Kaplan J, DeMaria M (2001) On the decay of tropical cyclone winds after landfall in the New England area. *J Appl Meteorol* 40:280–286
- Keim BD, Muller RA, Stone GW (2007) Spatiotemporal patterns and return periods of tropical storm and hurricane strikes from Texas to Maine. *J Climate* 20:3498–3509
- Khain A, Cohen N, Lynn B, Pokrovsky A (2008) Possible aerosol effects on lightning activity and structure of hurricanes. *J Atmos Sci* 65:3652–3677
- Levinson DH, Vickery PJ, Resio DT (2009) A climatology of landfalling hurricane central pressures along the Gulf of Mexico coast. In: Preprints, 11th International Workshop on Wave Hindcasting and Forecasting and 2nd Coastal Hazard Symposium, Halifax, Canada
- Lin N, Emanuel KA, Smith JA, Vanmarcke E (2010) Risk assessment of hurricane storm surge for New York City. *J Geophys Res*. doi:10.1029/2009JD013630
- Malmstadt JC, Elsner JB, Jagger TH (2010) Risk of strong hurricane winds to Florida cities. *J Appl Meteor Climatol* 49:2121–2132
- Mousavi ME, Irish JL, Frey AE, Olivera F, Edge BL (2010) Global warming and hurricanes: the potential impact of hurricane intensification and sea level rise on coastal flooding. *Clim Change*. doi:10.1007/s10584-009-9790-0
- Pearson AD, Sadowski AF (1965) Hurricane-induced tornadoes and their distribution. *Mon Weather Rev* 93:461–464
- Pielke RA Jr, Landsea CW (1999) La Niña, El Niño, and Atlantic hurricane damages in the United States. *Bull Amer Meteor Soc* 80:2027–2033
- Pielke RA Jr, Gratz J, Landsea CW, Collins D, Saunders MA, Musulin R (2008) Normalized hurricane damage in the United States: 1900–2005. *Nat Haz Rev* 9:29–42
- Powell MD, Houston SH (1998) Surface wind fields of 1995 hurricanes Erin, Opal, Luis, Marilyn, and Roxanne at landfall. *Mon Weather Rev* 126:1259–1273
- Scheitlin KN, Elsner JB, Malmstadt JC, Hodges RE, Jagger TH (2010) Toward increased utilization of historical hurricane chronologies. *J Geophys Res* 115, doi:10.1029/2009JD012424
- Schneider PJ, Schauer BA (2006) Hazus—its development and its future. *Nat Haz* 7:40–44
- Shay LK, Goni GJ, Black PG (2000) Effects of a warm oceanic feature on Hurricane Opal. *Mon Weather Rev* 128:1366–1383
- Simpson RH, Riehl H (1981) *The hurricane and its impact*. Louisiana State University Press, Baton Rouge
- Vickery PJ, Wadhera D (2008) Statistical models of Holland pressure profile parameter and radius to maximum winds of hurricanes from flight-level pressure and H\*Wind data. *J Appl Meteor and Climatol* 47:2497–2517
- Vickery PJ, Skerlj PF, Steckley AC, Twisdale LA (2000a) Hurricane wind field model for use in hurricane simulations. *J Struct Eng* 10:1203–1221
- Vickery PJ, Skerlj PF, Twisdale LA (2000b) Simulation of hurricane risk in the United States using empirical track model. *J Struct Eng* 10:1222–1237
- Vickery PJ, Lin J, Skerlj PF, Twisdale LA Jr, Huang K (2006a) HAZUS-MH hurricane model methodology. I: Hurricane hazard, terrain, and wind load modeling. *Nat Haz Rev* 7:82–93
- Vickery PJ, Skerlj PF, Lin J, Twisdale LA Jr, Young MA, Lavelle FM (2006b) Hazus-mh hurricane model methodology. II: Damage and loss estimation. *Nat Haz Rev* 7:94–103
- Watson CC, Johnson ME (2008) Integrating hurricane loss models with climate models. In: Diaz HF, Murnane RJ (eds) *Climate extremes and society*. Cambridge University Press, Cambridge, pp 209–224
- Zhu P (2008) Impact of land-surface roughness on surface winds during hurricane landfall. *Quart J Roy Meteor Soc* 134:1051–1057